AIN SHAMS UNIVERSITY
FACULTY OF ENGINEERING

Vol. 42, No. 1, March 31, 2007

SCIENTIFIC BULLETIN
Received on : 18/2/2007
Accepted on : 15/3/2007
pp. : 45-63

NONLINEAR ANALYSIS OF TUBULAR STEEL–CONCRETE COMPOSITE COLUMNS

OSAMA O. EL-MAHDY

ABSTRACT

Concrete-filled steel tube columns (CFT) are widely used in high-rise buildings, bridges, and heavily loaded structures. The confinement of concrete by transverse steel tube is effective in improving the ductility and strength of these composite columns. Current design codes tend to underestimate the ultimate strength of CFT columns. In this paper, an accurate modeling for CFT columns is achieved by using the nonlinear three-dimensional finite element method. Columns of circular, square, and rectangular cross-sections are considered. The confinement-sensitive concrete compression model and a suitable constitutive relationship are used for modeling the concrete core and the steel tube, respectively. The bond-slip between the steel tube and the concrete core is incorporated in the model. The results obtained from the proposed analytical model are compared with the measured ones obtained from the available experimental works that was conducted by other researchers. In addition, comparisons of strengths of CFT columns calculated using five different buildings codes and the present analytical model are given. The comparisons indicated that, the present model is accurate enough to predict the prepeak and postpeak behaviors as well as the strength of CFT columns. Furthermore, the proposed model may serve as a means to improve the design code formula for such columns.

KEYWORDS: Composite Columns; Confined Concrete; Nonlinear Finite Element Analysis; Bond; Constitutive Models; Experimental Results.

الملخص العربي:

في السنوات الأخيرة ازدادت تطبيقات الأعمدة المركبة من الحديد والخرسانة في منشآت المباني المرتفعة والكباري وذلك نظرا لما تتميز به هذه الأعمدة من خواص إنشائية ممتازة من حيث المقاومة القصوى والمرونة العالية, في هذا البحث تم اقتراح نموذج تحليلي للأعمدة المركبة والمكونة من ماسورة حديد مملؤة بخرسانة عادية. وقد تم استخدام طريقة العناصر المحددة والتحليل اللاخطي لنماذج من هذه الأعمدة, وقد تم تمثيل الخرسانة باستخدام نموذج الضغط المحاط الحساس كما تم تمثيل الماسورة الحديدية بطريقة دقيقة0 واستخدامت عناصر الالتصاق لتمثيل سطح التماس بين الماسورة الحديدية والخرسانة

[1] Associate Professor, Department of Civil Engineering, Faculty of Engineering at Shoubra, The University of Banha, Cairo 11629, EGYPT.

المالئة, وقد تم دراسة نتائج الدراسة التحليلية من حيث قيم المقاومـة القصوى, شكل التشكيلات والانبعـاج المحدد للماسورة الحديدية0 وقد قورنت هذه القيم بنتائج الدراسات المعملية بواسطة بـاحثون آخـرون ومـن ثم تم استنتاج أن النموذج المقترح يمثل سلوك هذه الأعمدة بدقة تامة وبالتالي يمكن الاعتماد على النموذج التحليلـي اللاخطـي فـي تطـوير معـادلات كـودات التـصميم لهـذه الأعمـدة بهـدف الحـصول علـى تـصميم اقتصادي0

1. INTRODUCTION

Composite columns composed of concrete-filled steel pipes or tubes (CFT) have become increasingly popular in structural applications around the world, especially in zones with high seismic activity. This type of columns can offer many advantages; for instance, high strength and stiffness, enhanced ductility and stability, and large energy absorption capacity, as well as increased speed of construction, positive safety aspects, and possible use of simple standardized connections. In addition, today's possibility to produce concrete with higher compressive strengths allows the design of more slender columns, which permits more usable floor space. In such hybrid columns, the steel tube interacts with the concrete core in three ways: (1) it confines the core, thereby enhancing its compressive strength and ductility; (2) it provides additional shear strength for the core; and (3) depending on its bonding strength with concrete and its stiffness in the axial direction, it develops some level of composite action, thereby also enhancing the strength of the concrete. The concrete core, in return, prevents the inward buckling of the steel tube.

Although the use of CFT columns is becoming more commonplace, concrete core confinement is not well understood. Confinement in a CFT column is continuous, unlike the conventional spiral reinforced concrete column. However, if the concrete core and the steel tube are loaded simultaneously, the steel tube expands more than the concrete core under moderate loads, since Poisson's ratio is higher for the steel section. This suggests that the steel tube may offer little confinement under certain conditions. Also, the high modulus of elasticity of the steel tube causes a large portion of axial loads to be carried by the tube, resulting in premature buckling. Current design specifications tend to underestimate the ultimate strength of CFT columns since the beneficent interactive confining effect between the steel tube and the concrete core is not totally considered.

While there have been many experimental studies of CFT columns, there has been fewer analytical work modeling the confining effect of the steel tube on the concrete. Mashaly et al. (2005) presented an analytical study on the behavior of concrete filled steel box columns. An equivalent uniaxial stress-strain relationship is used for concrete core. Drucker-Prager yield criterion is used to model the yield surface of concrete. For steel box, von-Mises yield criteria defined the yield surface, and Prandtl-Reuss flow rule was used to determine inelastic deformations. The obtained analytical results were compared with AISC/LRFD specifications. Also, a parametric study was carried out to investigate the effect of wall thickness, length of column, and type of concrete on the ultimate strength of composite columns. Saleh et al. (2005) conducted an experimental study to investigate the behavior of short double-skin concrete filled steel tube columns concentrically loaded up to failure. Six circular hollow sections for both outer and inner skins specimens were tested and the obtained experimental results were used to investigate the adequacy of some design specifications that are suited to CFT columns. Johansson and Gylltoft (2002) conducted an experimental and analytical study on the mechanical behavior of circular steel-concrete composite stub columns. Three loading conditions were studied to examine different mechanical behaviors of the columns. The established nonlinear analytical model was used to study how the behavior of the column was influenced by the bond strength between the steel tube and the concrete core and by the confinement of the concrete core offered by the steel tube. The results obtained from the tests and the finite-element analysis showed that the mechanical behavior of the column was greatly influenced by the method used to apply the load to the column section. The bond strength had no influence on the behavior when the steel and concrete sections were loaded simultaneously. On the contrary, for the columns with the load applied only to the concrete section, the bond strength highly affected the confinement effects and, consequently, the mechanical behavior of the columns. Abdel-Salam et al. (2001) presented an analytical formulation for the calculation of the idealized moment curvature relationships for circular concrete filled steel tube beam-columns. The proposed idealization is partially based on the observations from experimental study. The model is based on the von Mises yield criterion with an associated plastic flow rule for steel tube and the triaxial state of the confined concrete core. First yield and ultimate moments as well as their corresponding curvatures were predicted. Shams and Saadeghvaziri (1999) presented an evaluation of the nonlinear response of concrete-filled tubular columns subjected to axial loading. The von Mises elasto-plastic model with kinematic hardening was used for the steel tube. Pramano-Williams fracture energy-based model was used to model the concrete core. A parametric study was performed to identify the effect of different parameters such as width-wall thickness aspect ratio, length-width ratios, steel tube yield stress, and concrete uniaxial compressive stress. A total number of 63 square and 63 circular CFT coulumn were analyzed. Schneider (1998) conducted an experimental and analytical study on the behavior of short, concrete-filled steel tube columns. Depth-to-tube wall thickness ratios between 17 and 50, and the length-to-tube depth ratios of 4 to 5 were investigated. The unconfined uniaxial stress-strain curve for concrete core prior to yield was used. Beyond the ultimate strength, an adjusted curve according to the experimental results was used. For the steel tube, von Mises yield criteria defined the yield surface and Prandtl-Reuss flow rule determined inelastic deformations were used. The analytical study investigated the effect of the steel tube width or diameter-wall thickness aspect ratio on the load sharing between the concrete core and the steel tube.

The aim of this paper is to improve the current knowledge of the behavior of CFT columns subjected to axial loading and to make a more efficient use of high-strength concrete possible. To achieve this, a three-dimensional nonlinear finite-element analysis is conducted and verified with the available experimental results. The comparison shows that the proposed analytical model is accurate enough to predict the behavior of CFT columns in the elastic and plastic ranges. In addition, comparisons of the results obtained from the proposed model, experiment works, and five different buildings codes are given. A general purpose finite element program DIANA (ver. 9.1) was used in the nonlinear analysis. Predefined subroutines for the material properties are coded and implemented in the program. To this end, the rest of this research is organized as follows. First, the finite element modeling and nonlinear material models are presented. It is followed by a comparison of the results obtained from the analytical study and the experimental works. Next, the results obtained from different design codes are given. Finally, several conclusions are drawn.

2. FINITE ELEMENT MODELING

In the finite element model, the concrete core of the CFT column is modeled using twenty-node quadratic brick elements, with three degrees of freedom at each node. Eight-node shell elements, with five degrees of freedom at each node are used to model the steel tube. The formulation of shell elements allows large displacement analysis that is used to determine the possible initiation of local buckling for the steel tube. Gap contact element with sixteen-node is used for the interface between the concrete and steel components. The interface elements have no physical dimensions and thus they are used to connect two separate nodes occupying the same physical position. When the concrete and the steel tube are in contact with each other, normal and shear tractions are developed between the two materials. The coefficient of friction, μ, between concrete core and steel tube is set to 0.40. The concrete and steel are separated when the gab element is subjected to tension force. The finite element meshing for circular and square or rectangular CFT column is shown in Fig. 1. For the circular CFT columns, the mesh is mainly consists of twenty-node quadratic brick elements that match the geometry of the cylinder but a few are fifteen-node quadratic wedge elements. The external load is applied on the concrete core and steel tube simultaneously. The symmetrical arrangement of the column made it possible to select only one-eighth of the CFT column to be considered in the analysis. Appropriate boundary conditions are imposed on the symmetrical planes of the model.

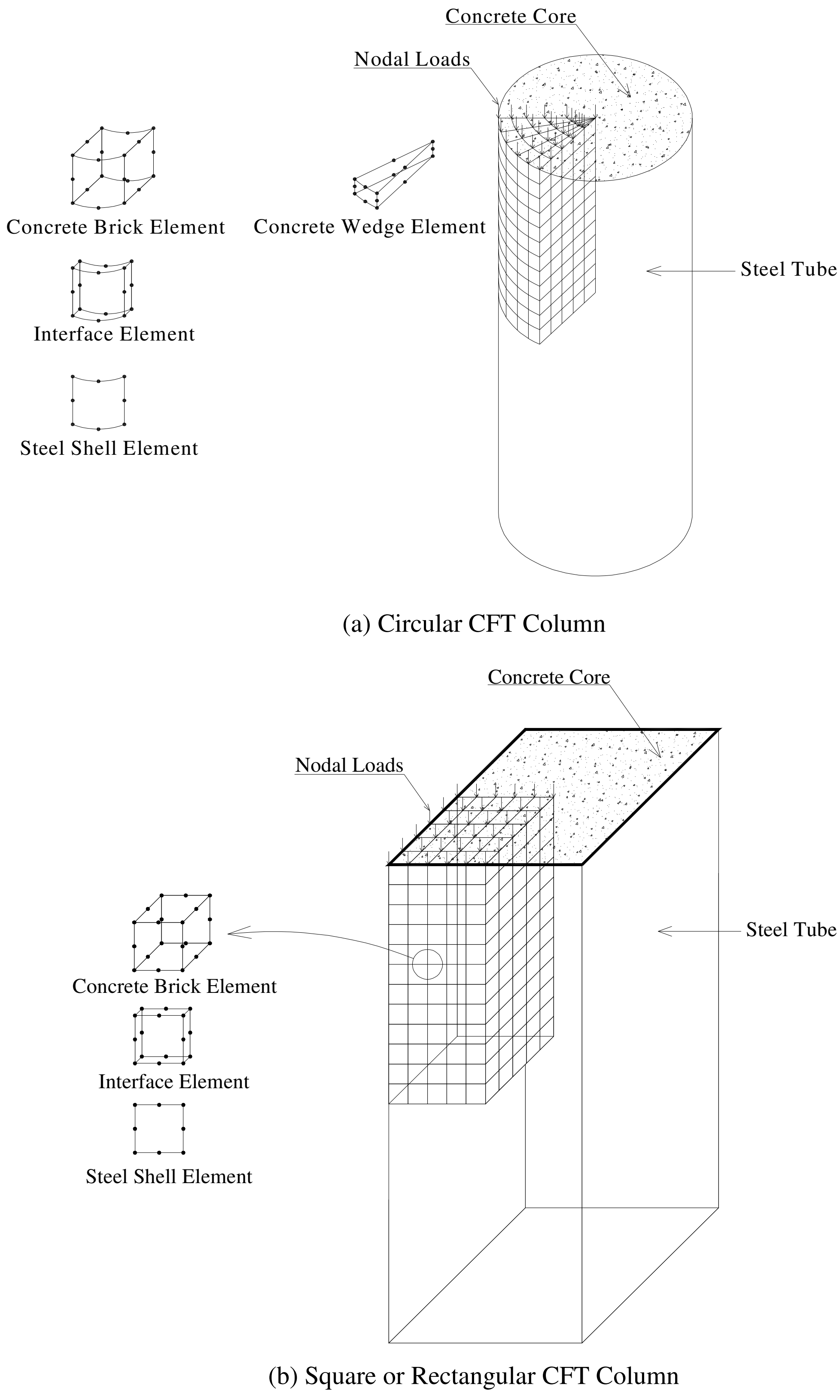

Fig. 1 Finite Element Meshing for One-Eighth of the CFT Column

3. MATERIALS MODELING

3.1 Concrete Model

The concrete core is characterized by triaxial compressive stress conditions with variable confining stresses. Therefore, the concrete can act as a quasi-brittle, plastic-softening, or plastic-hardening material depending on the confining stress. This is because under higher confining stresses the possibility of bond cracking is greatly reduced and the failure mode shifts from cleavage to crushing of cement paste. There are several approaches for modeling the complex behavior of the concrete that can yield reasonable solutions from an engineering point of view (Seow and Swaddiwudhipong (2005), Cuomo et al. (2004), De Borst (1997), Barzegar and Maddipudi (1997), and Etse and Willam (1994)). In this paper, the confinement-sensitive concrete compression model proposed by Johansson and Akesson (2003) is utilized. This model is fundamentally the Drucker-Parger model with the associated flow rule but it is extended to include a confinement-sensitive hardening behavior by means of two adjustment functions connected to the strength and the plastic modulus. The model has the following three components:

(a) The yield surface for the Drucker-Prager model which is a linear function in both the deviatoric stress q and the hydrostatic pressure p:

$$F(\sigma, K) = q + p\tan\alpha - K = 0 \tag{1}$$

where σ is the stress tensor, K is the strength repressing the cohesion, and α is the frictional angle.

(b) The associated flow rule component which express the evolution of plastic strains:

$$d\varepsilon^{P} = d\lambda\frac{\partial Q}{\partial\sigma} = d\lambda\frac{\partial F}{\partial\sigma} = d\lambda(\sqrt{\frac{3}{2}}\frac{S}{|S|} + \frac{\tan\alpha}{3}\delta) \tag{2}$$

where S is the deviatoric stress tensor, $d\lambda$ is the plastic multiplier, and δ is kronecker delta. Also, Q and F represent the plastic flow potential function and the yield criterion, respectively.

(c) The associated hardening rule which consists of two parts describing the evolution of the hardening parameter κ; and the strength hardening parameter dependence:

$$d\kappa = d\lambda\frac{\partial F}{\partial\kappa} = -d\lambda \qquad \textit{and} \qquad K = -Hd\lambda \tag{3}$$

where H is the isotropic hardening modulus. The true strength hyper-surface obtained from the calibration of pertinent triaxial test data is shown in Fig. 2. The confinement stress in any element is taken as the mean value of the two smallest principal stresses under the condition that it is compressive, otherwise it is set equal to zero. Furthermore, the friction angle α, was set to 30 degrees and the Poisson's ratio for the concrete in the elastic part was taken 0.20.

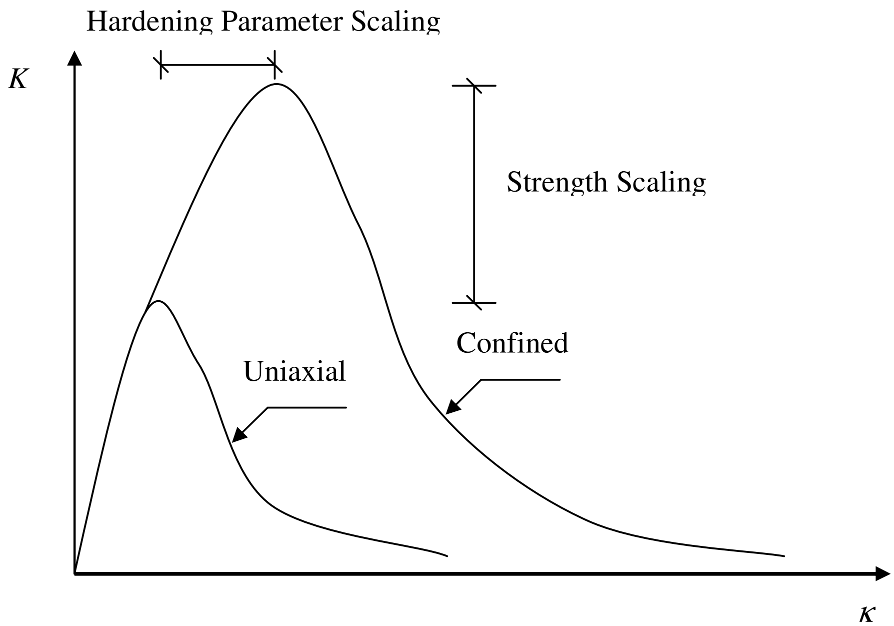

Fig. 2 Confined Strength-Hardening Parameter Relationship

3.2 Steel Model

The steel tube of a CFT column is in compression in the longitudinal and radial directions, and a tension in the hoop direction. Therefore, the inelastic action of the steel tube begins at a stress less than the yielding stress (Aboutaha and Machado, 1999). The constitutive relationship of steel tube that adapted to model the steel under triaxial stress are as follows (refer to Fig. 3):

$$\sigma_i = \frac{\sqrt{2}}{3}[(\sigma_x - \sigma_y)^2 + (\sigma_y - \sigma_z)^2 + (\sigma_z - \sigma_x)^2 + \frac{3}{2}(\tau_{xy}^2 + \tau_{yz}^2 + \tau_{zx}^2)]^{0.5} \quad (4)$$

$$\varepsilon_i = \frac{\sqrt{2}}{3}[(\varepsilon_x - \varepsilon_y)^2 + (\varepsilon_y - \varepsilon_z)^2 + (\varepsilon_z - \varepsilon_x)^2 + \frac{3}{2}(\gamma_{xy}^2 + \gamma_{yz}^2 + \gamma_{zx}^2)]^{0.5} \quad (5)$$

where

σ_κ = Normal stress in k direction , *k=x,y,z*;

ε_κ = Normal strain in k direction , *k=x,y,z*;

$\tau_{\kappa 1}$ = Shear stress in k-1 plane, *k=x,y,z; 1=x,y,z, and k≠1*;

$\gamma_{\kappa 1}$ = Shear strain in k-1 plane, *k=x,y,z; 1=x,y,z, and k≠1*;

f_y = Yielding stress of steel;

f_p = Proportional stress limit of steel;

f_u = Ultimate stress of steel under uniaxial tension.

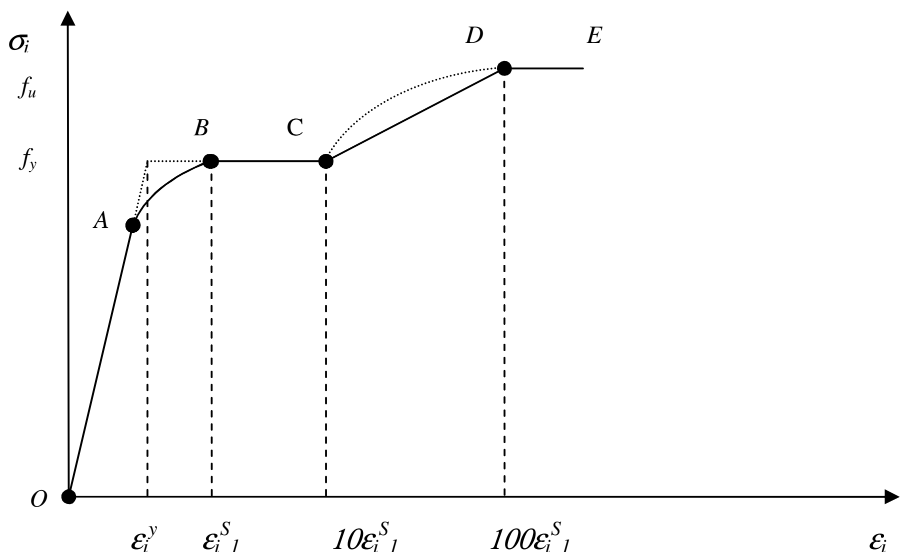

Fig. 3 Stress-Strain Relationship for Steel Tube

The σ_i-ε_i complete curve is divided into five stages: elastic (*OA*), elasto-plastic (*AB*), Plastic (*BC*), hardening (*CD*), and plastic flow (*DE*). Two simplified assumptions are adopted: a linear hardening is used to substitute the nonlinear hardening relationship and when the stress σ_i, reaches ultimate strength, f_u, which is in plastic failure flow stage, a horizontal flow (*DE*) is adopted to modify its behavior (Zhong and Zhang, 1993). Poisson's ratio in the elastic part was taken 0.30.

Before yielding of steel tube the utilized incremental stress-strain relationships is

$$d\{\sigma\} = [D]d\{\varepsilon\} \tag{6}$$

On the other hand, the plastic theory is employed after steel tube yields:

$$d\{\varepsilon\} = d\{\varepsilon^e\} + d\{\varepsilon^p\} \tag{7}$$

$$d\{\varepsilon^{p}\} = \lambda \frac{\partial \sigma_i}{\partial \{\sigma_i\}} \tag{8}$$

where

[D]	=	Tangent incremental modulus of steel before yielding;
$d\{\sigma\}$	=	Stress incremental matrix;
$d\{\varepsilon\}$	=	Strain incremental matrix;
$d\{\varepsilon^e\}$	=	Elastic strain incremental matrix;
$d\{\varepsilon^p\}$	=	Plastic strain incremental matrix;
λ	=	Scalar multiplier ($\lambda>0$).

4. NUMERICAL TECHNIQUE

A nonlinear analysis of the present model accounting for all important effects on internal stress distribution, crack propagation, external deformations, bond between the steel tube and the concrete core, and local buckling of the steel tube can only be realized by a step-by-step solution procedure. The Modified Newton-Raphson technique is therefore, utilized in the present analysis. In this method, the external load is applied incrementally, but after each increment successive iterations are performed to satisfy equilibrium and constitutive relations within each load increment.

A sufficient number of iterations are allowed during the analysis until a converged solution is reached. The nonlinear analysis is carried out using ether energy or force controlled convergence criterion. The obtained results are almost the same for both criteria; however the running time for force controlled analysis was about 60% of that for energy controlled analysis. In force controlled analysis, the convergence is attained when the maximum residual nodal forces are less than a user-specified tolerance, which is defined as a small fraction of the applied nodal forces. In case of either singularity or non-convergence problems are encountered, the load step size is reduced. Then, the solution is restarted from the encountered load value. Before each new load step, the tangential stiffness matrix is updated.

5. ANALYTICAL RESULTS AND DISCUSSIOIN

In order to verify the applicability and accuracy of the proposed model, the load-deformation relationships, initiation of steel tube local buckling, and effect of confinement level on the overall load carrying capacity are obtained and compared with the experimental results that conducted by other researchers (Tan et al. (2005), Schneider (1999), and Fukuzawa et al. (1987)).

5.1 Load-Deformation Relationship

Figure 4 show the compression between the results obtained using the present analytical model and those measured experimentally. Different shapes of circular, square, and rectangular steel tubes are considered. The steel to total composite area ratios, $A_s/(A_s+A_c)$ are 8.3%, 9.5%, and 11.3% for circular, square, and rectangular specimens, respectively. The width-wall thickness aspect ratios, D/t are shown in the figure. The length-width ratios for all specimens are ranging from 4.0 to 4.80. Other details of the test specimens and the material mechanical properties can be found in Schneider (1999). Good agreement between the analytical and experimental results in both elastic and plastic behavior is observed. The circular CFT columns show strain hardening type of behavior. On the other hand, the degrading type of behavior is observed in both square and rectangular CFT columns in which there is a deterioration of axial capacity after the peak load. It should be mentioned here that, in the case of square and rectangular CFT columns the obtained stress distributions along the cross-section are not uniform. The center and the corners of the sections go under a higher confining pressure than the sides. Where as, in the case of circular CFT columns the axial and lateral stress distributions are radially uniform.

5.2 Local Buckling of Steel Tube

The comparison between the experimental and analytical initiation of steel tube local buckling at midheight plane for square CFT columns having various width-wall thickness aspect ratios, D/t, is illustrated in Fig. 5. In general, the square tube shapes exhibited post-yield behavior depending on the tube wall thickness. For D/t=40.3 and 27.9, the specimens are classified as strain-softening behavior. On the other hand, for $D/t=17$ the specimen is classified as strain-hardening behavior. In all specimens, local buckling of steel tube did not occur prior to yield of the CFT column. Moreover, higher axial deformations are obtained, prior to local wall buckling, for the thicker steel tubes. This figure shows that the aspect ratio D/t has a significant effect on the strength, ductility, and local buckling of the steel tube. As the ratio D/t is increased, strength and ductility are decreased and the predicted steel tube local buckling is occurred at a point far away from the peak load. Furthermore, a ductile behavior is observed even after local buckling has occurred. Again the results of the nonlinear analysis and experimental work are in good agreement.

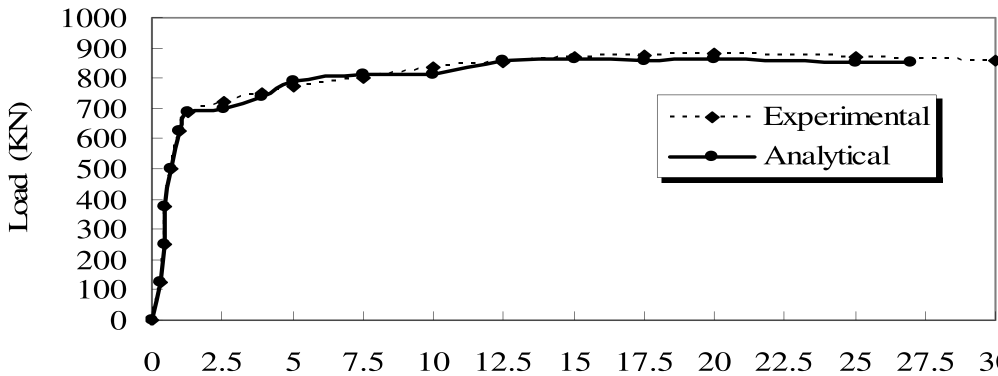

(a) Circular CFT Column D/t=46.7

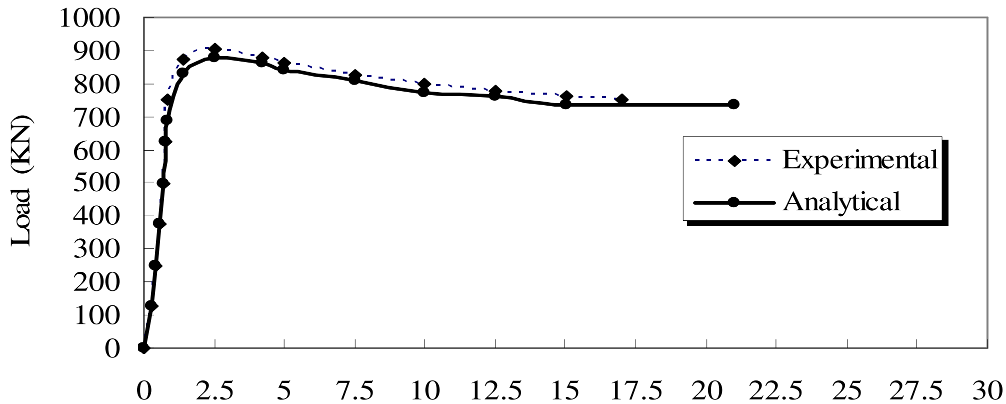

(b) Square CFT Column D/t=40.3

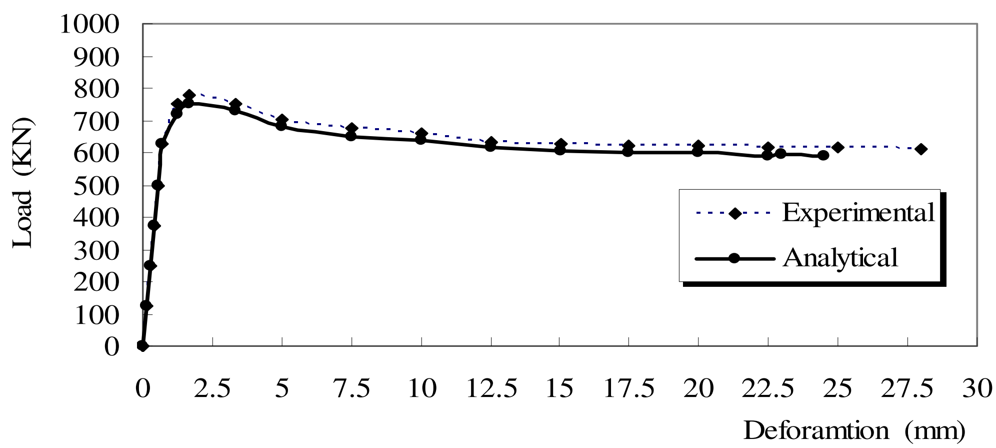

(c) Rectangular CFT Column D/t=50.7

Fig. 4 Load-Deformation Relationships for Different Shapes of CFT Columns

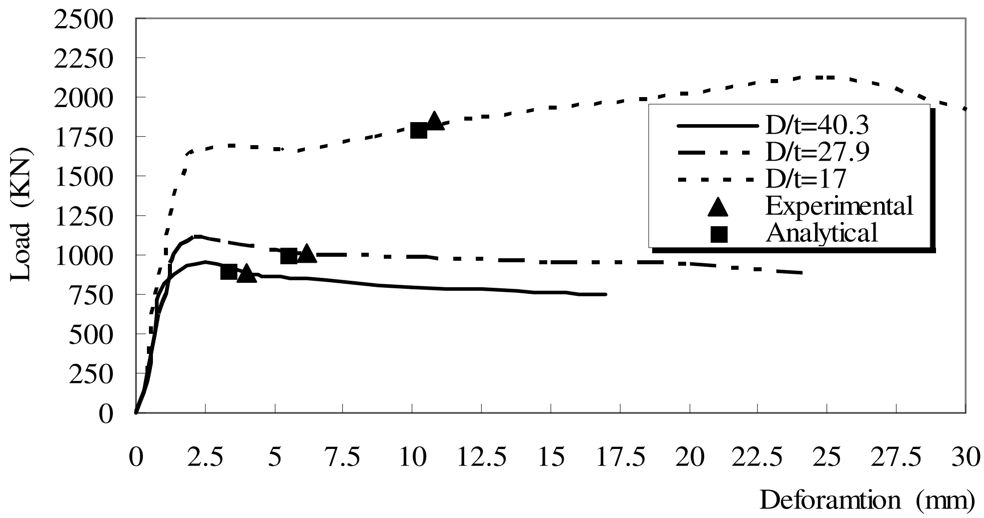

Fig. 5 Initiation of Local Buckling for Square CFT Columns Having Different Aspect Ratios (*D/t*)

5.3 Confinement Level and the Load Carrying Capacity of CFT Columns

The experimental measured strengths of CFT columns having different confinement degrees and those calculated using the proposed model is listed in Table 1. The details of the test arrangements, concrete properties, and steel tube dimensions and properties are found in Tan et al. (2005). The comparison shows that, the analytical model is able to simulate the effect of the aspect ratio *D/t*, on the ultimate strength of CFT columns. The *D/t* ratio for specimen ST-A represents the extreme condition that exceed the ratio limits cited in codes provisions. Also, the concrete compressive strengths for all specimens are higher than the restricted values given by design codes.

Table 1 Experiment and Analytical Load Carrying Capacity of Circular CFT Columns

Specimen No.	*D/t*	θ	Capacity (KN)		A/E
			Experimental (E)	Analytical (A)	
ST-A	125	0.09	1258	1214	0.965
ST-B	63.5	0.20	1414	1319	0.984
ST-C	38	0.46	1985	1908	0.961
ST-D	28.3	0.66	2229	2115	0.949
ST-G	18.15	1.33	3379	3170	0.938

θ is the confinement index given by Eq. (28).

6. COMPARISON WITH BUILDING CODES AND STANDARS

This chapter is devoted to compare the results predicted by different design provisions for CFT columns against the experimental data from other researchers as well as the results calculated using the present analytical model. The following sections summarize five codes of practice for the design of concrete-filled steel circular tube columns.

6.1 AISC-LRFD Code Provisions

In the AISC Load and Resistance Factor Design Code (AISC-LRFD, 1994), the compressive strength calculations for CFT columns are the same as for bare steel structural members with the exception that the modified properties F_{my}, E_m, and r_m are used. The axial design strength, P_n, is calculated as

$$\phi_c P_n = 0.85 A_s F_{cr} \tag{9}$$

where 0.85=value of the resistane factor for compression, ϕ_c, and the critical column stress, F_{cr} is

$$F_{cr} = (4.538^{\lambda_c^2}) F_{my} \qquad for \qquad \lambda_c^2 \le 2.25 \tag{10}$$

$$F_{cr} = (\frac{6.048}{\lambda_c^2}) F_{my} \qquad for \qquad \lambda_c^2 > 2.25 \tag{11}$$

$$\lambda_c^2 = (\frac{KL}{\pi r_m})^2 \frac{F_{my}}{E_m} \tag{12}$$

where r_m is the modified radius of gyration about the axis of buckling. The AISC specifies that r_m should be taken as the radius of gyration of the steel tube alone, but not less than 30% of thickness of gross composite section in the plane of buckling. The modified yield stress, F_{my}, and the modified modulus of elasticity, E_m are defined as:

$$F_{my} = F_y + \frac{0.85 f_c' A_c}{A_s} \tag{13}$$

$$E_m = E_s + \frac{0.40 E_c A_c}{A_s} \tag{14}$$

It should be noted that for $\lambda = 0$, the strength equation becomes

$$\phi_c P_n = 0.85(A_s F_y + 0.85 A_c f_c') \tag{15}$$

which means that the capacity of a concrete-filled steel column is taken as the sum of the strength of its parts.

6.2 Eurocode (EC4) Provisions

In Eurocode 4 (1994), the plastic axial resistance, N_p of a circular concrete-filled steel column is given as

$$N_p = \frac{A_c f_{ck}}{\gamma_c}\left[1+\eta_1(\frac{t}{D})\frac{f_y}{f_{ck}}\right]+\eta_2\frac{A_s f_y}{\gamma_s} \tag{16}$$

where A_c and A_s = cross-sectional areas for concrete core and steel tube; γs and γc = partial safety factors for steel and concrete; and η_1 and η_2 = values that, respectively, increase the uniaxial compressive strength of the concrete due to confinement and reduce the yielding strength of the steel due to biaxial stresses.

The elastic critical load, N_{cr} is given by

$$N_{cr} = \frac{\pi^2 (EI)_e}{L^2} \tag{17}$$

where L= buckling length, and $(EI)_e$ = equivalent modulus of composite column calculated as the sum of individual components

$$(EI)_e = E_s I_s + 0.60 E_c I_c \tag{18}$$

where I_s and I_c = second moments of area for the steel tube and uncracked concrete core, respectively; E_s = elastic modulus for structural steel; and E_c = secant modulus of elasticity for short term loading of concrete.

The nondimensional slenderness factor, λ is defined as

$$\lambda = \sqrt{N_p / N_{cr}} \le 2.0 \tag{19}$$

where λ is no greater that 0.5 and M_f is no greater than $N_f(D/10)$, where M_f and N_f are the applied moment and axial load, respectively. The member is determined to have sufficient resistance if $N_f \le \chi N_p$, where the instability coefficient, χ is given by

$$\begin{aligned} \chi &= f_k - \sqrt{(f_k{}^2 - \lambda^{-2})} \le 1.0 \\ f_k &= 0.5\lambda^{-2}\left[1+0.21(\lambda-0.20)+\lambda^2\right] \end{aligned} \tag{20}$$

The values of η_1 and η_2 are given by

$$\begin{aligned} \eta_1 &= 4.9 - 18.5\lambda + 17\lambda^2 \ge 0 \\ \eta_2 &= 0.25(3+2\lambda) \le 1.0 \end{aligned} \tag{21}$$

6.3 British Standards Institution

The British Standards BS 5400 (1999) give the concrete contribution factor α_c, by

$$\alpha_c = \frac{0.45 f_{cc} A_c}{N_u} \tag{22}$$

and the squash load N_u is

$$Nu = 0.91 f_y' A_s + 0.45 f_{cc} A_c \tag{23}$$

where

f_{cc} = is an enhanced characteristic strength of triaxially contained concrete under axial load, given by:

$$f_{cc} = f_{cu} + C_1 \frac{t}{D_e} f_y \quad \text{,and} \tag{24}$$

f'_y = is a reduced nominal yield strength of the steel casing, given by:

$$f_y' = C_2 f_y \tag{25}$$

where

C_1 and C_2 = Constants given in the code
D_e = The outside diameter of the steel tube
t = The wall thickness of the steel casing
and the remaining symbols are defined as before.

6.4 Chinese Specifications

According to the Chinese Specifications for the Design and Construction of CFT columns (Cai, 1993), the ultimate load carrying capacity can be calculated as follows:

$$N_u = \phi_l \phi_e N_o \tag{26}$$

where ϕ_l=strength reduction factor due to slenderness ratio, ϕ_e= strength reduction factor due to eccentricity, and N_o= squash load of concentrically-loaded short column computed by

$$N_o = A_c f_c (1 + \sqrt{\theta} + \theta) \tag{27}$$

where:

$$\theta = \frac{A_s f_s}{A_c f_c} \tag{28}$$

in which θ is the confinement index; A_c is the cross-sectional area of concrete; f_c is the design compressive strength of concrete core; A_s is the cross-sectional are of steel tube; and f_s is the design strength for the steel tube.

6.5 Egyptian Code of Practice

The Egyptian Code of Practice (2006) gives the following formulae for the design of columns made of CFT (Article 10.2.3):

$$P = A_s F_c \tag{29}$$

$$F_c = (0.58 - \alpha F_{ym} \lambda^2) F_{ym} \quad for \quad \lambda \le 100 \tag{30}$$

$$Fc = 3.57 \frac{E_m}{\lambda^2} \quad for \quad \lambda \ge 100 \tag{31}$$

where:

$$F_{ym} = F_y + 0.68 f_{cu} (A_c / A_s) \tag{31}$$

$$E_m = E_s + 0.40 E_c (A_c / A_s) \tag{32}$$

$$\alpha = (0.58x10^4 F_{ym} - 3.57 E_m) / (10^4 F_{ym})^2 \tag{33}$$

$$\lambda = Kl / r_m \tag{34}$$

$$r_m = r_s \tag{31}$$

in which F_c is the allowable compressive axial stress of the steel section, Kl is the buckling length.

Table 2 Comparison of the Measured and Computed Ultimate Loads

Specimen	Ultimate Load (KN)						
	Measured	Present Model	Design Code				
			AISC	EC4	BS 5400	Chinese	ECC
CFT-2.3	1815	1712	1121	1107	1113	1389	729*

* Allowable working load.

Table 2 shows the load design capacity for CFT circular columns calculated using different codes of practice as well as the present analytical model. Also, the experimental average measured value for three specimens that were conducted by Fukuzawa et al. (1987) are given. From this comparison, it can be noted that the measured ultimate load of CFT column exceeds the calculated permissible value using the Egyptian code with a factor of safety of 2.5. Furthermore, the AISC, EC4, and BS5400 Design Codes give a lower estimate value compared with the Chinese Code. Close agreement between experimental and analytical values is observed.

7. CONCLUSIONS

Both steel structures and concrete structures always compete with the combined steel and concrete structures. It has been widely known that concrete-filled steel tubular (CFT) columns have much higher strength and deformation capacities than common reinforced concrete (RC) columns because of beneficent interactive confinement effect between the filled concrete and the steel tube. The confinement effect by the steel tube furthermore contributes to improving ductility of concrete, and enables application of CFT columns in high-rise buildings located in seismic regions. This paper describes a proposed three-dimensional nonlinear finite element model for studying the behavior of CFT columns. Columns of square, rectangular, and circular cross-sections are considered in this study. The confinement-sensitive concrete compression model and an appropriate constitutive relationship are utilized for modeling the filled concrete and steel tube, respectively. Interface elements are used to model the bond between concrete core and steel tube at the interface. The results obtained from the present model are compared with those either measured experimentally or calculated using five different building codes. The comparison shows that the present finite element model is accurate enough to model the behavior of CFT columns. Furthermore, the proposed model may serve as a means to improve the design code formulae with a view to achieving a safe and economic design for CFT columns.

REFERENCES

[1] Mashaly, E.S., Allan, S., El-Heweity, M., and Ibrahim, M., (2005), “Finite Element Analysis of Axially Loaded Concrete Filled Steel Box Columns”, Proceedings of the Eleventh International Colloquium on Structural and Geotechnical Engineering (11th ICSGE), Ain Shams University, Cairo, Egypt, E05ST 25-1 to 10.

[2] Saleh, A.A., Khalil, A.H.H., and Abel Wahed, O.H., (2005), “Response of Concrete Filled Double Skin steel Tube Columns to Axial Loads”, Proceedings of Eleventh International Colloquium on Structural and Geotechnical Engineering (11th ICSGE), Ain Shams University, Cairo, Egypt, E05RC 29-1 to 16.

[3] Johansson, M., and Gylltoft, K., (2002), "Mechanical Behavior of Circular Steel-Concrete Composite Stub Columns", Journal of Structural Engineering, ASCE, Vol. 128, No. 8, pp. 1073-1081.

[4] Abdel-Salam, M.N, Abdel-Ghaffar, M., and Zaki, M.A.G., (2001), " Flexural Capacity of Circular Concrete Filled Steel Tubes - An Analytical Model - Parts 1 and 2", Proceedings of Ninth International Colloquium on Structural and Geotechnical Engineering (9th ICSGE), Ain Shams University, Cairo, Egypt.

[5] Shams, M. and Saadeghvaziri, M.A., (1999), "Nonlinear Response of Concrete-Filled Steel Tubular Columns under Axial Loading", ACI Structural Joural, Vol. 96, No. 6, pp. 1009-1017.
[6] Schneider, S.P., (1998), "Axially Loaded Concrete-Filled Steel Tubes", Journal of Structural Engineering, ASCE, Vol. 124, No. 10, pp. 1125-1138.
[7] DIANA 9.1 "Finite Element Analysis", TNO Buildings and Construction Research, Netherlands.
[8] Seow, P.E.C. and Swaddiwudhipong, S., (2005), "Failure Surface for Concrete under Multiaxial Load – a Unified Approach", Journal of Materials in Civil Engineering, ASCE, Vol. 17, No. 2, pp. 219-228.
[9] Cuomo, M., Contrafatto, L., and Nicolosi, A., (2004), "Multiaxial Stress Analysis of Elastic-Plastic Damaging Concrete structures", Proceedings of European Congress on Computational Methods in Applied Sciences and Engineering (ECCOMAS 2004), pp. 1-20.
[10] De Borst, R., (1997), "Some Recent Developments in Computational Modeling of Concrete Fracture", International Journal of Fracture, Vo. 86, pp. 5-36.
[11] Barzegar, F. and Maddipudi, S., (1997), "Three-Dimensionl Modeling of Concrete Structures. I: Plain Concrete", Journal of Structural Engineering, ASCE, Vol. 123, No. 10, pp. 1339-1346.
[12] Etse, G. and Willam, K., (1994), "Fracture Energy Formulation for Inelastic Behavior of Plain Concrete", Journal of Engineering Mechanics, ASCE, Vol. 120, No. 9, pp. 1983-2011.
[13] Johansson, M. and Akesson, M., (2003), "Finite Element Study of Concrete-Filled Steel Tubes Using a New Confinement-Sensitive Concrete Compression Model", Publications No. 27 of Nordic Concrete Research (NCR), pp. 1-20.
[14] Aboutaha, R.S. and Machado, R.I., (1999), "Seismic Resistance of Steel-Tubed High-Strength Reinforced-Concrete Columns", Journal of Structural Engineering, ASCE, Vol. 125, No. 5, pp. 485-494.
[15] Zhong, S.T. and Zhang, S., (1993), "A new Method from China to Determine Load – Carrying Capacity for CFST Members", Proceedings of an Engineering Foundation Conference on Composite Construction in Steel and Concrete II; Edited by W. Samuel Easterling and W.M. Kim Roddis, Published by the ASCE, pp. 449-511.
[16] Tan, K., Nichols, J.M., and Pu, X., (2005), "Mechanical Properties of High Strength Concrete Filled Steel Tubular Columns: Part 1 – Concentrically Loaded Short Columns", Journal of Southwest University of Science and Technology, Natural Science Edition, Vol. 20, No.3 , pp. 27-54.
[17] American Institute of Steel Construction (AISC). (1994). Load and Resistance Factor Design – Manual of Steel Construction. Second Edition, Chicago, U.S.A.

[18] Eurocode 4 (1994) – Design of Composite Steel and Concrete structures, Part 1.1: General Rules and Rules for Buildings, CEN, Brussels.
[19] British Standards Institution. BS 5400: Part 5: 1979 & 1999: “Steel, Concrete, and Composite Bridges”, Code of Practice for Design of Composite Bridges.
[20] Cai, S.H., (1993), "Chinese Standard for Concrete-Filled Tube Columns", Proceedings of an Engineering Foundation Conference on Composite Construction in Steel and Concrete II; Edited by W. Samuel Easterling and W.M. Kim Roddis, Published by the ASCE, pp. 142-151.
[21] Egyptian Code of Practice for Steel Construction and Bridges (Allowable Stress Design), No. 205, Edition-2006.
[22] Fukuzawa, K., Numao, T., Hanata, K., Kiyota, S. (1987), "Axial Strength of Hollow Steel-Pipe-Concrete Composite Members", Transactions of Japan Concrete Institute (JCI), Vol. 9, pp. 381-388.